# Effect of N-Substituents on Redox, Optical, and Electronic Properties of Naphthalene Bisimides Used for Field-Effect Transistors Fabrication

**Pawel Gawrys,[†] David Djurado,[‡] Ján Rimarčík,[§] Aleksandra Kornet,[†] Damien Boudinet,[||] Jean-Marie Verilhac,[||] Vladimír Lukeš,[§] Ireneusz Wielgus,[†] Malgorzata Zagorska,*[,†] and Adam Pron*[,‡]**

*Faculty of Chemistry, Warsaw University of Technology, Noakowskiego 3, 00 664 Warszawa, Poland, INAC/SPrAM, UMR 5891 CEA-CNRS-Univ. J. Fourier-Grenoble 1, Laboratoire d'Electronique Moléculaire Organique et Hybride, 17 Rue des Martyrs, 38054 Grenoble Cedex 9, France, Institute of Physical Chemistry and Chemical Physics, Slovak University of Technology in Bratislava, SK-81 237 Bratislava, Slovakia, and CEA/LITEN/LCI, 17 Rue des Martyrs, 38054 Grenoble Cedex 9, France*

*Received: September 15, 2009; Revised Manuscript Received: December 24, 2009*

Three groups of naphthalene bisimides were synthesized and comparatively studied, namely, alkyl bisimides, alkylaryl ones, and novel bisimides containing the alkylthienyl moiety in the N-substituent. The experimental absorption spectra measured in $CHCl_3$ exhibit one intensive absorption band that is uniformly detected in the spectral range of 340 to 400 nm for all studied molecules. This band consists of three or four vibronic peaks. The introduction of an alkylthienyl group results in the appearance of an additional band (in the spectral range from 282 to 326 nm, depending on the position of the substituent) that can be ascribed to the $\pi-\pi^*$ transition in the thienyl chromophore. The minimal substituent effect on the lowest electronic transitions was explained using the quantum chemical calculations based on the time-dependent density functional theory. The investigation of the shapes of frontier orbitals have also shown that the oxidation of bisimides containing thiophene moiety is primary connected with the electron abstraction from the thienyl ring. To the contrary, the addition of an electron in the reduction process leads to an increase in the electron density in the central bisimide core. As shown by the electrochemical measurements, the onset of the first reduction potential (so-called "electrochemically determined LUMO level") is sensitive toward the type of the substituent being shifted from about −3.72 eV for bisimides with alkyl substituents to about −3.83 eV for alkylaryl ones and to about −3.94 eV for bisimides with thienyl groups. The presence of the thienyl ring also lowers the energy difference between the HOMO and LUMO orbitals. These experimental data can be well correlated with the DFT calculations in terms of HOMO/LUMO shapes and energies. Taking into account the low position of their LUMO level and their highly ordered supramolecular organization, the new bisimides are good candidates for the use in n-channel field effect transistors, operating in air. The fabricated "all organic" transistors show effective charge carrier mobilities in the range $10^{-2}$ to $10^{-4}$ $cm^2$ $V^{-1}$ $s^{-1}$ and the ON/OFF ratios exceed $10^5$ for the majority of cases.

## Introduction

Arylene bisimide derivatives are promising materials for organic or molecular electronics and more specifically for the fabrication of n-channel field-effect transistors. However, their application in this field is frequently impeded by several factors of physicochemical or technological nature. It has been experimentally established that air operating n-channel field effect transistors (FETs) require the use of bisimides whose LUMO level is below 3.95−4.0 eV with respect to the vacuum level.[1] Arylene bisimides with alkyl N-substituents do not fulfill this condition,[2] and the lowering of their LUMO levels necessitates core or imide group functionalization with an electron withdrawing group.[3] Core functionalization is chemically complicated, whereas N-functionalization usually involves the introduction of perfluorinated substituents that have a strongly negative effect on the bisimide solution processability. In our previous paper[4] we have demonstrated that in naphthalene bisimides, that is, bisimides of the smallest core, the LUMO level is sensitive to even relatively small changes in the electron withdrawing/electron donating properties of the N-substituent. For example, the replacement of an alkyl substituent by an aryl one lowers the LUMO level by 70−150 meV. No effect of this type is observed for larger core bisimides. Thus, tuning of the LUMO level position can be achieved, in this case, by the use of much milder electron acceptors that in addition do not perturb the bisimide solution processability.

Having in mind the above-discussed features, we have undertaken the task of systematic investigations, both experimental and theoretical, of the N-substituent effect on these properties of naphthalene bisimides that are of fundamental importance for their application in organic electronics. This involves the determination of their redox, optical, and electronic properties, elucidation of their supramolecular organization in thin layers, as well as the fabrication of test transistors. In particular, the following groups of solution processable compounds have been compared: alkyl, alkylaryl, alkylthienylaryl,

* Corresponding author. E-mail: zagorska@ch.pw.edu.pl; adam.pron@cea.fr.
[†] Warsaw University of Technology.
[‡] INAC/SPrAM.
[§] Slovak University of Technology in Bratislava.
[||] CEA/LITEN/LCI.

10.1021/jp908931w 
Published on Web 01/19/2010

and alkylthienyl bisimides. The last two groups, never reported in the literature, have been synthesized for the purpose of this research.

## Experimental Section

The description of the synthetic procedures used for the preparation of alkyl and alkylaryl naphthalene bisimides, together with their spectroscopic data (NMR, FTIR, and elemental analysis) can be found in ref 4. The same information concerning bisimides containing alkylthienyl groups is given in Supporting Information.

X-ray diffraction studies were performed on a X-Pert Pro MPD Philips diffractometer (cobalt $K_{\alpha 1}$ radiation; $\lambda = 1.789$ Å) in the Bragg−Brentano ($\theta/2\theta$) reflection geometry. The detector was moved by $2\theta$ steps of 0.02° and the counting time was 12 s per step. Soller slits were mounted both in the incident beam path (0.04 rad) and in the diffracted beam path (0.01 rad). It should be pointed out that the registered widths of Bragg peaks were limited by the resolution. As a consequence, some of them were split off due to the presence of the back Soller slit; accordingly, a fixed receiving slit of 0.03125° was added to avoid this problem. With such an experimental setup the positions of the Bragg peaks could be determined with good accuracy but not their relative intensities. The degree of orientation order of the (001) Bragg peak was also evaluated by performing an omega scan ($\omega = \theta_0 \pm \Delta\omega$).

Solution spectra of the bisimides dissolved in chloroform were recorded on a Varian Cary 5000.

Electrochemical studies were carried out in a one-compartment, three-electrode electrochemical cell containing $10^{-3}$ M solution of a given bisimide in 0.1 M $Bu_4NBF_4/CH_2Cl_2$ electrolyte. The measurements were performed using an Autolab potentiostat (Eco Chemie) with a platinum working electrode of the surface area of 3 mm$^2$, a platinum mesh counter electrode, and an Ag/0.1 M $Ag^+$/acetonitrile reference electrode. The potential of the reference versus $Fc/Fc^+$ redox couple was checked at the end of each experiment.

All organic test transistors (Cytop dielectric) were prepared on a poly(ethylene naphthalate) (PEN) substrate using commercially available Cytop as the dielectric layer. Details concerning their fabrication can be found in Supporting Information.

## Calculation Details

The electronic ground state geometries of the studied systems were optimized using Density Functional Theory (DFT)[5] based on the Becke's three parameter hybrid functional using the Lee, Yang, and Parr correlation functional for Gaussian (B3LYP).[6] Based on the optimized geometries, the vertical transition energies and oscillator strengths between the initial and final states were computed by a time-dependent version (TD-) of the DFT method.[7] The 6-31G* basis set has been used[8] and the calculations were done using the Gaussian 03 program package.[9] The energy cutoff was of $10^{-3}$ kcal mol$^{-1}$ and the final root-mean-square energy gradient was under 0.01 kcal mol$^{-1}$ Å$^{-1}$. The obtained optimal structures were checked by normal-mode analysis (no imaginary frequencies for all optimal geometries). The numerical integration of the used functional was performed using the fine integration grid which parameters are set as default. Due to the extreme computational requirements, our theoretical model was restricted to a single molecule without taking any solvent or temperature effects into account as a standard simplification used in quantum chemical studies.

**CHART 1: Chemical Structures of the Studied Bisimides**

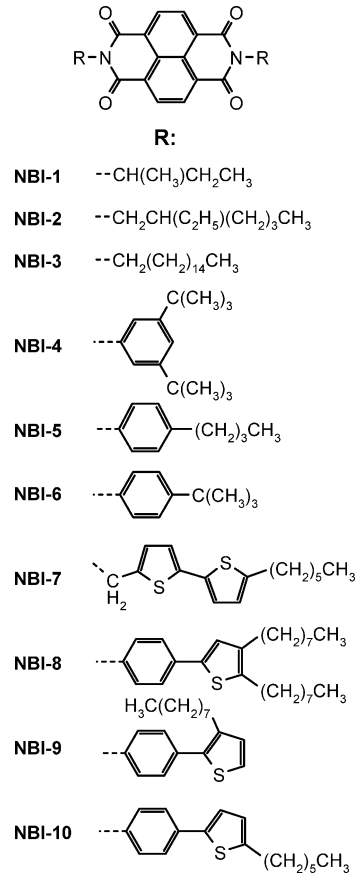


## Results and Discussion

Arylene bisimides are very sensitive toward core functionalization. Introducing an electron withdrawing group to their core results in lowering of their LUMO[1,3] level and profound changes of their UV−vis spectra.[10] These changes are observed even for rather mildly electron accepting moieties directly linked to the aromatic core like bithiophene groups, as it has been reported for many functionalized bisimides, including alternating copolymers of naphthalene or perylene bisimides and bithiophene.[11] To the contrary, the sensitivity of bisimides of larger core size toward the electron accepting/donating properties of the N-substituent is less pronounced. Small changes in the electron accepting/donating properties of the N-substituent, for example, the replacement of an alkyl substituent by an aryl one does not influence the LUMO level of perylene or larger core bisimides to a significant extent.[12] In this respect, the smallest core arylene bisimides, that is, naphthalene bisimides, behave differently. It has been demonstrated that naphthalene bisimides with N-alkylaryl substituents show lower lying LUMO levels by 80−130 meV as compared to the corresponding N-alkyl bisimides.[4] This observation opens up a new possibility for the electronic properties tuning in naphthalene bisimide-based organic semiconductors. Therefore, this paper is devoted to the experimental and theoretical analysis of the substituent effect in differently N-functionalized naphthalene bisimides. The three groups of compounds studied, namely, naphthalene bisimides with alkyl, alkylaryl, and alkylthienylaryls substituents, are presented in Chart 1.

All synthesized bisimides are suitable for the preparation of field effect transistors by solution processing. However, they differ in their solubility in solvents used for processing such as

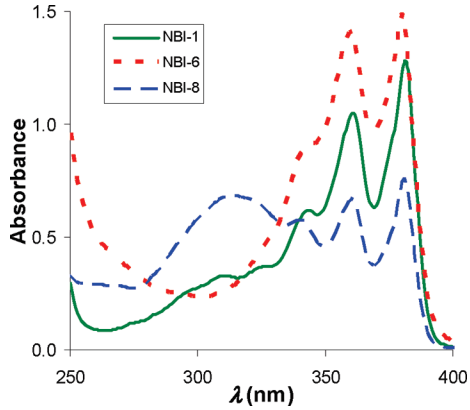


**Figure 1.** UV−vis spectra recorded of **NBI-1**, **NBI-6**, and **NBI-8** dissolved in chloroform.

chloroform, methylene chloride, dichlorobenzene, and others. In general, bisimides with alkyl substituents show better solubility than those with alkylaryl ones. The solubility of bisimides containing alkylthienyl moiety is regiochemically predetermined. **NBI-8** and **NBI-9** show excellent solubility comparable to that observed for bisimides with alkyl substituents. Lower solubility is observed for **NBI-10** in which the alkyl chain is attached in the α position. This type of substitution minimally affects the $\pi$-stacking and facilitates the alkyl chains interdigitation. These two phenomena are probably the principal cause of the reduced solubility.

UV−vis spectra of all naphthalene bisimides show a characteristic band at about 380 nm associated with their core $\pi-\pi^*$ transition (see Figure 1).[13] A pronounced vibronic structure can clearly be seen with the 0→0 vibronic peak of the lowest electronic transition being the most intensive. The equidistant energy difference (0.18 eV) between the vibronic peaks indicates a harmonic character of the vibrational motion. In the spectral range studied, the differences between bisimides with alkyl substituents and those with alkylaryl ones are minimal, which means that the effect of the substituent is restricted to the imide group and does not extend to the aromatic core. The introduction of an alkylthienyl group as an inherent part of the substituent results in the appearance of an additional band, which can be ascribed to the $\pi-\pi^*$ transition in the thienyl chromophore being in conjugation either with the adjacent phenyl ring (**NBI-8**, **NBI-9**, and **NBI-10**) or with the adjacent, second thienyl ring (**NBI-7**). Spectroscopic data collected in Table 1 unequivocally indicate that the extent of this conjugation depends on the position of the alkyl group in the thienyl ring. The presence of this group in the 3-position of the thienyl ring lowers the effective conjugation between the two aromatic systems, which is manifested by a hypsochromic shift of the $\pi-\pi^*$ chromophore band. This can be clearly seen by a comparison of the spectroscopic data of **NBI-9** and **NBI-10**, where the thienyl chromophore peaks appear at 282 and 311 nm, respectively. Still some local conjugation between the thienyl and phenyl rings in **NBI-9** exists because the $\pi-\pi^*$ transition band in an isolated thienyl ring gives rise to a peak at about 240 nm.[14]

It is instructive to compare the experimentally measured spectra with the calculated ones. It should be noted that the presence of single bonds connecting the substituents with the central bisimide part leads to a large number of possible conformations. Therefore, we have restricted our calculations only to these conformations where the opposite mutual arrangement of the neighboring lateral rings is not parallel. As has been recently shown, these conformations exhibit the lowest total energies for the ladder type molecules with respect to the steric conditions.[15] In the optimal geometries, the studied molecules are planar in their central part. The orientation of the lateral aromatic rings and the bisimide skeleton is nearly perpendicular. For the alkylaryl substituents, the torsion between these rings is 80 to 90°, depending on the position of the alkyl group. For the alkylthienylaryl derivatives, these dihedral angles are lower, that is, 72° for **NBI-8**, 73° for **NBI-9**, and 84° for **NBI-10**. The mutual orientation between the phenylene and thiophene fragments is 25−28°, the highest being calculated for **NBI-9**, as expected from the spectroscopic measurements (vide supra). The torsion angles between the planar bisimide skeleton and the phenylene ring in the substituent are responsible for the very limited $\pi$-conjugation between these molecular fragments.

The selected, lowest calculated electronic transitions with dominant oscillator strengths are collected in Table 1. The theoretical values of the lowest optical transition for the isolated molecules are slightly shifted from the experimental ones by 5−16 nm, however, the agreement between the experiment and the theory is good. Our calculations indicate a negligible substituent effect on the lowest optical transition, which also agrees with the experimental observations. The absence of the dominant transitions in the discussed range 340−400 nm indicates that the shape of the first band has the vibronic character. The second lowest calculated transition, occurring in the range 302−315 nm in bisimides with alkyl substituents,

**TABLE 1: Experimental and Theoretical Optical Parameters Obtained for Naphthalene Bisimides Studied in this Research**[a]

| | experimental (nm) | | theoretical (nm) |
|---|---|---|---|
| compound | $\lambda_{max}$ (core) | $\lambda_{max}$ (subst) | $\lambda_{max}$ (calcd) |
| **NBI-1** | 381, 361, 343, 323[b], 312[b] | | 369 (0.350), 311 (0.095) |
| **NBI-2** | 381, 361, 342, 323[b], 311[b] | | 368 (0.327), 315 (0.087) |
| **NBI-3** | 381, 361, 343, 323[b], 312[b] | | 368 (0.338), 314 (0.080) |
| **NBI-4** | 381, 361, 343 | [c] | 367 (0.452), 302 (0.069) |
| **NBI-5** | 381, 360, 343 | [c] | 365 (0.417), 303 (0.087) |
| **NBI-6** | 381, 360, 343 | [c] | 366 (0.427), 302 (0.083) |
| **NBI-7** | 381, 360, 339 | 326 | 383 (0.104), 370 (0.533), 322 (0.973), 321 (0.274), 300 (0.050) |
| **NBI-8** | 381, 360, 340 | 314 | 367 (0.725), 351 (0.080), 300 (1.381) |
| **NBI-9** | 380, 360, 343 | 282 | 367 (0.532), 327 (0.087), 297 (0.060), 275 (0.112), 274 (0.487), 274 (0.193) |
| **NBI-10** | 380, 360, 340 | 311 | 367 (0.624), 342 (0.084), 294 (1.341), 292 (0.139) |

[a] The experimental values are separated into the contributions of bisimide moiety (core) and substituents. The calculated transitions for $\lambda_{max}$ (calcd) larger than 270 nm with dominant oscillator strengths (in parentheses, $f > 0.05$) are presented in the last column. [b] Weak and distinguishable only for N-alkyl substituted bisimides (see Figure 1). [c] The $\pi-\pi^*$ transition of aromatic ring for aryl substituent overlaps with naphthalene core band at ca. 237 nm (ref 14).

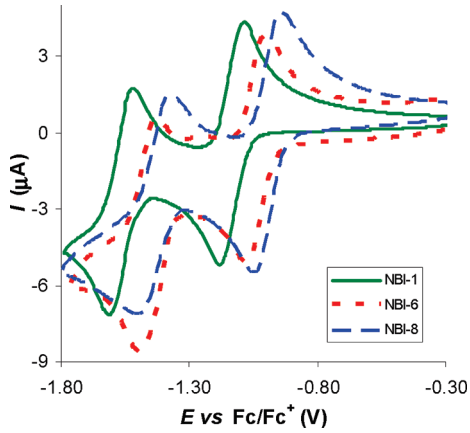


**Figure 2.** Cyclic voltammograms of **NBI-1**, **NBI-6**, and **NBI-8**. Scan rate of 100 mV/s; electrolyte 0.1 M $Bu_4NBF_4$ in $CH_2Cl_2$; concentration $10^{-3}$ M.

shows small but not negligible oscillator strength. This is in agreement with the experimental measurements where a small band appears in this spectral region. Its vibrational structure is unresolved (see Figure 1). For the thienyl ring containing bisimides, the calculations reveal the presence of an intensive transition in the spectral range from 274 to 322 nm, originating from the presence of an additional chromophore. In accordance with the experiment, the most energetic transition (274 nm) was found for **NBI-9** (see Table 1).

To identify the origin of the vibronic structure detected in the optical spectra, the calculated vibration spectrum for the smallest investigated molecule **NBI-1** was analyzed. As seen in Table 1S (see Supporting Information), the calculated vibrational spectrum starts from the frequency of 23 $cm^{-1}$, corresponding to lateral ring torsions, ring deformations and in plane bending of the whole aromatic system with small intensities. Many of the calculated modes include in- and out-of-plane CH and CC bending torsional vibrations and CC ring stretches (see peaks in the region between 800 and 1800 $cm^{-1}$). In accordance with the plethora of experimental data, the theoretical aromatic CH-stretch vibrations are located at about 3200 $cm^{-1}$. The most intensive vibrational modes, connected with the C−C stretches within the aromatic core, are depicted in Figure 1S. A reasonable correspondence of the theoretical modes of the largest intensities (1101, 1282, 1358 and 1736, 1774 $cm^{-1}$) with the averaged experimental value of 0.18 eV (1452 $cm^{-1}$) indicate that these motions are responsible for the vibronic structure present in all spectra of the studied molecules.

Spectroscopic studies seem to indicate that the core $\pi-\pi^*$ transition in naphthalene bisimides is not very dependent on the N-substituent. One may, however, expect that the imide part of the molecule will be more affected by its chemical nature. This can be conveniently verified by cyclic voltammetry, taking into consideration the well-known mechanism of arylene bisimide reduction.[12] According to this mechanism, the reduction reaction is a two step process involving the reduction of the carbonyl group to a radical anion followed by the formation of a spinless dication in the second step. Thus, the cyclic voltammetry gives rise to two redox couples, which, in the case of naphthalene bisimides, are clearly separated. Figure 2 shows representative cyclic voltammograms obtained for the three groups of naphthalene bisimides studied, whereas the electrochemical parameters of all bisimides studied are listed in Table 2.

As seen from Figure 2 and from the data collected in the last column of Table 2, bisimides with alkyl substituents are the most difficult to reduce. Alkylaryl bisimides undergo electrochemical reduction at higher potentials, whereas bisimides containing thienyl groups are the most easy to reduce. The observed behavior can be rationalized by the fact that the presence of an additional aromatic ring of electron accepting properties, next to imide nitrogen, lowers the charge density at the reduction site through its additional delocalization, facilitating in this manner the first reduction process and stabilizing the resulting radical anion. This effect is even more pronounced in substituents containing phenyl and thienyl rings with $\pi$ systems being in conjugation. Note that this increase of the first reduction potential is also observed for **NBI-7** where the thienyl ring is separated from the imide nitrogen by a methylene linker.

The positions of the electrochemical LUMO levels with respect to the vacuum level were obtained from the onset of the first reduction peak using the following formulas[16]

$$\text{LUMO} = -\text{e} \times (E_{\text{red1(onset)}} + 4.8)\ \text{eV} \quad \text{and}$$
$$\text{HOMO} = -\text{e} \times (E_{\text{ox(onset)}} + 4.8)\ \text{eV} \qquad (1)$$

For all molecules, the HOMO levels were obtained by subtraction of the optical gap from the electrochemically determined LUMO ($1240/\lambda_{\text{offset}}$, where $\lambda_{\text{offset}}$ of the core $\pi-\pi^*$ optical transition (390 nm)). Only for bisimides containing the thienylene moiety the HOMO level was additionally determined electrochemically from the onset of the oxidation peak.

From the obtained data, summarized in Table 3, it is clear that the replacement of alkyl substituents by alkylaryl ones in naphthalene bisimides shifts the electrochemical LUMO level in the proper direction as far as the fabrication of air operating n-channel FETs is considered. This effect is even more pronounced in the case of alkylthienylaryl or alkylbithienylmethylene substituents.

In this context, it is useful to examine the shapes of theoretically calculated HOMO and LUMO orbitals of the investigated molecules, which play an important role in the spectroscopic as well as electrochemical processes. They are shown in Figure 3.

**TABLE 2: Electrochemical Parameters Obtained for Naphthalene Bisimides Studied in this Research: *E* versus $Fc/Fc^+$**

| compound | $E_{\text{red1}}$/V | $E_{\text{ox1}}$/V | $E_{\text{red2}}$/V | $E_{\text{ox2}}$/V | $^1/_2(E_{\text{red1}} + E_{\text{ox1}})$/V | $E_{\text{red1(onset)}}$/V |
|---|---|---|---|---|---|---|
| **NBI-1** | −1.18 | −1.10 | −1.60 | −1.53 | −1.140 | −1.08 |
| **NBI-2** | −1.15 | −1.06 | −1.58 | −1.49 | −1.105 | −1.03 |
| **NBI-3** | −1.14 | −1.05 | −1.54 | −1.46 | −1.095 | −1.03 |
| **NBI-4** | −1.09 | −1.01 | −1.51 | −1.44 | −1.050 | −0.99 |
| **NBI-5** | −1.07 | −1.00 | −1.49 | −1.42 | −1.035 | −0.98 |
| **NBI-6** | −1.07 | −1.00 | −1.49 | −1.42 | −1.035 | −0.97 |
| **NBI-7** | −1.05 | −0.96 | −1.46 | −1.35 | −1.01 | −0.88 |
| **NBI-8** | −1.05 | −0.94 | −1.50 | −1.37 | −0.99 | −0.86 |
| **NBI-9** | −1.06 | −0.94 | −1.55 | −1.36 | −1.00 | −0.86 |
| **NBI-10** | −1.06 | −0.95 | −1.56 | −1.40 | −1.01 | −0.86 |

**TABLE 3: Positions of Theoretical and Experimental LUMO and HOMO Levels**

| | experimental | | | theoretical | |
|---|---|---|---|---|---|
| compound | LUMO[a] | HOMO[b] | HOMO[c] | LUMO[d] | HOMO[d] |
| **NBI-1** | −3.72 | −6.90 | | −3.07 | −6.93 |
| **NBI-2** | −3.77 | −6.95 | | −3.11 | −6.97 |
| **NBI-3** | −3.77 | −6.95 | | −3.09 | −6.96 |
| **NBI-4** | −3.81 | −6.99 | | −3.03 | −6.70 |
| **NBI-5** | −3.82 | −7.00 | | −3.03 | −6.68 |
| **NBI-6** | −3.83 | −7.01 | | −3.01 | −6.47 |
| **NBI-7** | −3.92 | −7.10 | −5.51 | −3.44 | −5.33 |
| **NBI-8** | −3.94 | −7.12 | −5.73 | −3.31 | −5.53 |
| **NBI-9** | −3.94 | −7.12 | −6.04 | −3.39 | −5.88 |
| **NBI-10** | −3.94 | −7.12 | −5.89 | −3.32 | −5.65 |

[a] Determined from the onset of the first reduction peak using eq 1. [b] Determined by subtracting the optical gap from electrochemically determined LUMO level, as LUMO-1240/$\lambda_{offset}$, where $\lambda_{offset}$ = 390 nm. [c] Determined from the onset of the oxidation peak using eq 1. [d] B3LYP/6-31G* calculations.

For alkyl and alkylaryl bisimides, the HOMO-to-LUMO transition contributes significantly to the lowest excitation energy. This contribution ranged from 60 to 95%. Lower contributions (40−45%) were obtained for alkylthienylaryl and alkylthienyl bisimides. From the electrochemical point of view, the shape of frontier orbitals can indicate from which part of the molecule the electron is abstracted upon oxidation or the electron is added upon the reduction. As it can be seen in Figure 3, the shapes of HOMO orbitals are dependent on the type of lateral substituent. The HOMO orbitals of alkyl or alkylaryl derivatives are uniformly delocalized only over the central part. The lobes of these orbitals are perpendicularly oriented to the aromatic chain. The energetically degenerated HOMO orbitals of the alkylthienylaryl and alkylthienyl compounds are delocalized over the thiophene moieties. The LUMO orbitals show the inter-ring bonding character and their lobes are spread along the central part for all investigated compounds. The calculated values of HOMO and LUMO energies of the molecular orbitals at DFT theoretical level for the optimal B3LYP/6-31G* geometries are also collected in Table 3 and their relative values are shown in Figure 2S (see Supporting Information).

In the case of bisimides containing thienyl groups, a large discrepancy can be found between the positions of the HOMO level determined by the subtraction of the optical gap from the electrochemically determined LUMO level and the calculated ones. This can be explained by the fact that the HOMO energy values listed in column 2 of Table 3 contain other contributions than those originating from the pure HOMO orbital. To the contrary, the values of the electrochemically determined HOMO levels are in good agreement with the theoretical calculations, indicating that the removal of the electron occurs at the thienyl ring (see shapes of HOMO orbitals in Figure 3).

All bisimides studied are suitable candidates for the fabrication of organic transistors by solution processing. Bisimides with substituents containing thienyl groups deserve, however, a special attention because the positions of their LUMO levels approach the values recommended for air operating FETs.[1] A good compound, for transistor application, in addition to the requirements of the thermodynamic nature, should exhibit a specific supramolecular organization that favors charge carriers transport. Naphthalene bisimides are sometimes polymorphic and may show different structures, depending on processing conditions. It has been demonstrated, for example, that **NBI-1** adopts a herringbone structure in single crystals, whereas in thin layers deposited on poly(ethylene naphthalate) or Si substrates

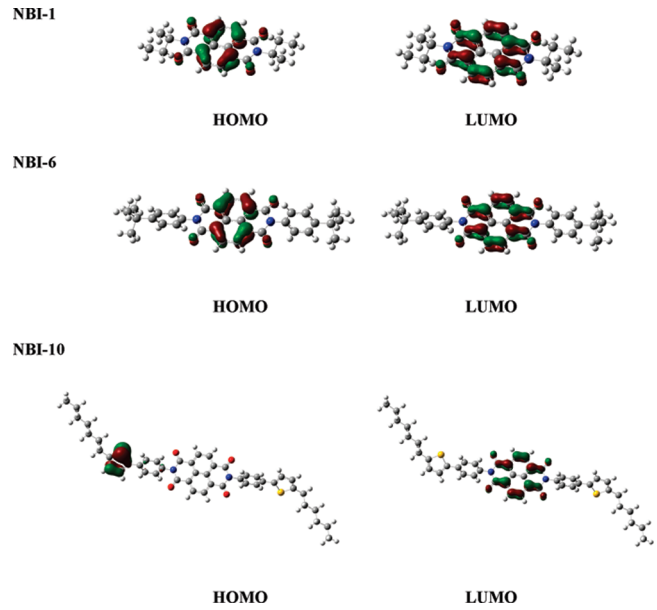


**Figure 3.** Plots of the B3LYP/6-31G* HOMO and LUMO for the **NBI-1**, **NBI-6**, and **NBI-10** molecules.

it exhibits a $\pi$-stacked molecular organization, which is more favorable for the charge transport.[4] We have therefore undertaken the task of the structural order elucidation in thin layers of naphthalene bisimides of the same thickness as those spin-coated in the transistor fabrication process.

A similar type of structural organization can be found in thin layers of the synthesized naphthalene bisimides. First, it should be noted that the deposited layers are crystalline. Among them, however, the case of **NBI-8** seems to be the most instructive, showing a remarkably well developed diffraction pattern (Figure 4a). For this reason, the model structure of this bisimide will be discussed here as an example, however, the drawn conclusions can be extended to other bisimides of the three families investigated.

First, it should be noted that in the diffractogram of **NBI-8** a long period with additional high order diffraction peaks, indexed as (00L) can be found. This finding is consistent with a lamellar-like structure with a parameter of 25.7 Å. However, the length of the fully extended molecule can be estimated to be about 44 Å, a much higher value than that measured for the long period. Based on these two parameters, a simple model can be proposed in which parallel $\pi$-stacked molecules stand on the substrate with a tilt angle of 45−66°, with respect to the substrate. The exact value of this angle depends on the extent of alkyl tails interdigitation, as illustrated in Figure 4b, where this model structure is schematically depicted.

The next question to be answered is the degree of the orientation of crystalline domains of imide molecules with respect to the substrate. This can be done by performing so-called omega scan at the respective $2\theta$ positions of the most intense Bragg peak, which in the case of **NBI-8** is $2\theta = 4.00°$. The results are shown in Figure 5.

The obtained profile consists of an extremely narrow peak superimposed on a very large one. It can therefore be postulated that in a thin layer of the bisimide highly oriented crystalline domains coexist with nonoriented ones. From the FWHM value of the narrow peak, a very small orientation distribution of the oriented crystalline domains is obtained corresponding to 0.046°.

If the crystalline order is considered in relation to the chemical structure of the investigated bisimides, it must be inferred that

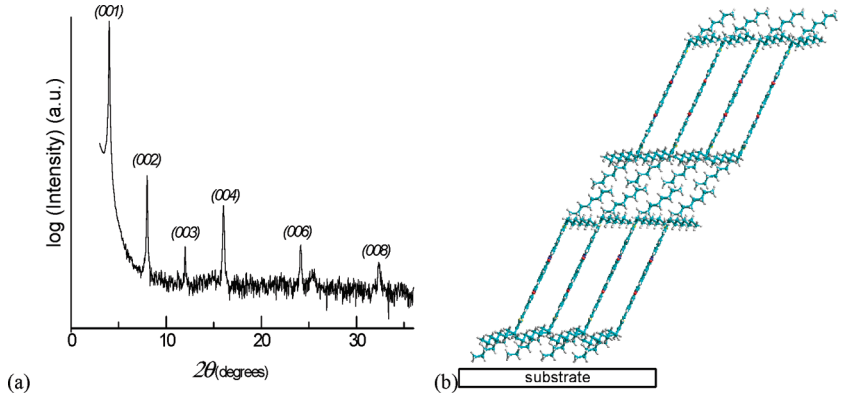


**Figure 4.** (a) X-ray profile of **NBI-8** deposited on untreated ⟨100⟩ Si substrate, obtained in Bragg−Brentano reflection geometry. (b) Model of possible stacking mode in thin layers of **NBI-8**.

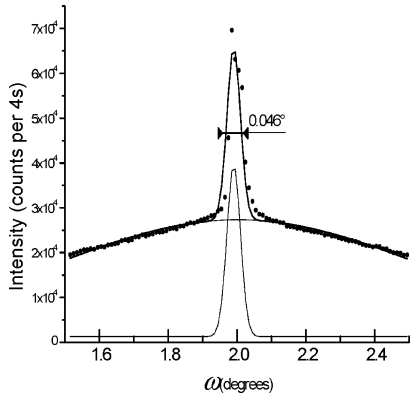


**Figure 5.** Omega scan obtained around the Bragg position of the (001) line of **NBI-8**.

$\pi$-stacking of the aromatic parts and interdigitation of the end alkyl groups constitute the driving force for the formation of large and remarkably well oriented crystalline domains. It must also be stressed that this orientation can be obtained using simple solution processing techniques such as spin coating or casting without the necessity of application of external, orientation inducing stimuli.

The above-described results were obtained for films deposited on silicon substrates, whereas the test transistors were fabricated on poly(ethylene naphthalate) (PEN). Detailed investigations of this type could not be performed for bisimide films deposited on PEN due to the fact that the strong diffraction profile of polycrystalline PEN completely masked the principal reflections

**TABLE 4: Electrical Parameters of Transistors Fabricated from Naphthalene Bisimides Studied in this Research**

| compound | $\mu$/cm$^2$ V$^{-1}$ s$^{-1}$ | ON/OFF | $V_T$/V |
|---|---|---|---|
| **NBI-1** | $4.0 \times 10^{-2}$ | $4.5 \times 10^5$ | 35 |
| **NBI-2** | $6.4 \times 10^{-3}$ | $5.5 \times 10^3$ | 45 |
| **NBI-5** | $2.4 \times 10^{-4}$ | $1.5 \times 10^3$ | 46 |
| **NBI-6** | $4.0 \times 10^{-4}$ | $2.5 \times 10^4$ | 49 |
| **NBI-7** | $9.1 \times 10^{-3}$ | $5.0 \times 10^5$ | 18 |
| **NBI-8** | $6.4 \times 10^{-3}$ | $2.4 \times 10^5$ | 57 |

originating from the deposited bisimide. In our previous study,[4] we have however demonstrated, using the grazing incidence geometry, that the molecular organization in thin layers of **NBI-1**, deposited on Si or PEN, is essentially the same, although small differences in the orientation distribution and the crystallite size may exist. This similarity is not unexpected because the strong tendency to self-organize via $\pi$-stacking and alkyl end groups interdigitation should easily overcome the effect of the substrate.

The synthesized bisimides were used for the fabrication of all organic test transistors. In Table 4, electrical parameters measured for the prepared FETs are collected, whereas their representative output and transfer characteristics are shown in Figure 6.

Among three groups of naphthalene bisimides tested, those containing alkylthienyl moiety in their N-substituents deserve a special attention (see Tables 2 and 3). First, they show lower lying LUMO levels by 170 to 220 meV as compared to the case of alkyl naphthalene bisimides, which is, of course, favorable for the fabrication of FETs operating under ambient

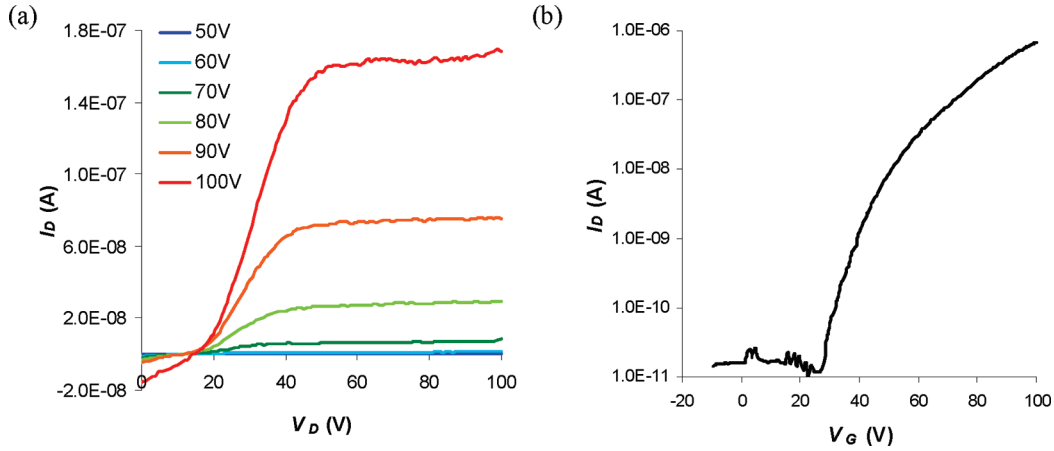


**Figure 6.** Output (a) and transfer (b) characteristics of a typical OFET fabricated from **NBI-8**.

conditions. This lowering of the LUMO levels has been achieved through a relatively simple chemistry (see Supporting Information). Second, their compact structural organization, determined for thin solid layers, favors charge transport. As a result, transistors with good electrical parameters can be fabricated. Third, the synthesized bisimides are solution processable. This last property is technologically advantageous because it makes possible the fabrication of organic FETs in which, apart from the evaporation of source and drain electrodes, all other depositions are made by spin-coating or printing techniques. Arylene bisimide-based, all-organic transistors, that is, transistors with an organic semiconductor and an organic gate dielectric, prepared by solution processing, are still scarce,[4,16d,17] but their importance increases due to the technological simplicity of their fabrication. Finally, it should be noted that some of the fabricated transistors reach the state of the art for all organic FETs prepared by solution processing.

## Conclusions

To summarize, by combining theoretical and experimental investigations, we have demonstrated that naphthalene bisimides, contrary to the case of larger core bisimides, are very sensitive to even small changes in the electron accepting/electron donating properties of their N-substituents. The replacement of alkyl substituents by alkylaryl ones or by substituents containing alkylthienyl groups makes possible precise tuning of the LUMO level position in the range from −3.72 to −3.94 eV with respect to the vacuum level. The synthesized bisimides are solution processable and can be used for the fabrication of all organic n-channel field effect transistors by spin-coating or printing techniques. The DFT calculations showed that the $\pi$-conjugation between the lateral aromatic rings and planar central part is perturbed. Therefore, the lowest optical transitions exhibit practically uniform values for all studied molecules. Based on the normal-mode analysis, the dominant vibrations that are responsible for the vibronic structure of optical spectra were also identified. The investigation of the shapes of the frontier orbitals shows that the oxidation of naphthalene bisimides containing thiophene moiety in their N-substituent proceeds via the abstraction of an electron from the thienylene ring. To the contrary, the reduction of the bisimide leads to an increase of the electron density in the central part of the molecule.

**Acknowledgment.** We acknowledge financial support from Polish Ministry of Science and Higher Education through Research Project NN205105735 in years 2008−2011 and Bilateral French−Polish Cooperation Project "Polonium" No. 7822/R09/R10. This work has been supported also by Slovak Grant Agency VEGA (Projects No. 1/0774/08) and the Science and Technology Assistance Agency (Bilateral French-Slovak Cooperation Project PHC 2008/2009, 17956ZD/ SK-FR 0001-07). Researchers from Grenoble acknowledge the participation in European project Network of Excellence POLYNET.

**Supporting Information Available:** Synthesis of all novel bisimides containing thienyl moieties; fabrication of field effect transistors (FETs); total electronic energies; fully optimized Cartesian coordinates for studied systems; and the calculated B3LYP normal modes for the smallest molecule, **NBI-1**. This material is available free of charge via the Internet at http://pubs.acs.org.

## References and Notes

(1) Jones, B. A.; Facchetti, A.; Wasielewski, M. R.; Marks, T. J. *J. Am. Chem. Soc.* **2007**, *129*, 15259–15278.

(2) Katz, H. E.; Johnson, J.; Lovinger, A. J.; Li, W. *J. Am. Chem. Soc.* **2000**, *122*, 7787–7792.

(3) (a) Jones, B. A.; Facchetti, A.; Marks, T. J.; Wasielewski, M. R. *Chem. Mater.* **2007**, *19*, 2703–2705. (b) Wang, Z.; Kim, C.; Facchetti, A.; Marks, T. J. *J. Am. Chem. Soc.* **2007**, *129*, 1336213363;(c) Jones, B. A.; Ahrens, M. J.; Yoon, M.-H.; Facchetti, A.; Marks, T. J.; Wasielewski, M. R. *Angew. Chem., Int. Ed.* **2004**, *43*, 6363–6366. (d) Chen, H. Z.; Ling, M. M.; Mo, X.; Shi, M. M.; Wang, M.; Bao, Z. *Chem. Mater.* **2007**, *19*, 816824. (e) Li, Y.; Tan, L.; Wang, Z.; Qian, H.; Shi, Y.; Hu, W. *Org. Lett.* **2008**, *10*, 529532. (f) Weitz, R. T.; Amsharov, K.; Zschieschang, U.; Villas, E. B.; Goswami, D. K.; Burghard, M.; Dosch, H.; Jansen, M.; Kern, K.; Klauk, H. *J. Am. Chem. Soc.* **2008**, *130*, 4637–4645. (g) Schmidt, R.; Ling, M. M.; Oh, J. H.; Winkler, M.; Könemann, M.; Bao, Z.; Würthner, F. *Adv. Mater.* **2007**, *19*, 3692–3695. (h) Jones, B. A.; Facchetti, A.; Wasielewski, M. R.; Marks, T. J. *Adv. Funct. Mater.* **2008**, *18*, 1329–1339. (i) Yan, H.; Zheng, Y.; Blache, R.; Newman, C.; Lu, S.; Woerle, J.; Facchetti, A. *Adv. Mater.* **2008**, *20*, 3393–3398. (j) Piliego, C.; Jarząb, D.; Gigli, G.; Chen, Z.; Facchetti, A.; Loi, M. A. *Adv. Mater.* **2009**, *21*, 1573–1576. (k) Piliego, C.; Cordella, F.; Jarzab, S.; Lu, S.; Chen, Z.; Facchetti, A.; Loi, M. A. *Appl. Phys. A* **2009**, *95*, 303–308.

(4) Gawrys, P.; Boudinet, D.; Zagorska, M.; Djurado, D.; Verilhac, J.-M.; Horowitz, G.; Pécaud, J.; Pouget, S.; Pron, A. *Synth. Met.* **2009**, *159*, 1478–1485.

(5) Parr, R. G.; Yang, W. *Density-Functional Theory of Atoms and Molecules in Chemistry*, Springer-Verlag: New York, 1991.

(6) Becke, A. D. *J. Chem. Phys.* **1993**, *98*, 5648.

(7) Furche, F.; Ahlrichs, R. *J. Chem. Phys.* **2002**, *117*, 7433.

(8) (a) Petersson, G.; Al-Laham, M. *J. Chem. Phys.* **1991**, *94*, 6081–6090. (b) Rassolov, V.; Ratner, M.; Pople, J.; Redfern, P.; Curtiss, L. *J. Comput. Chem.* **2001**, *22*, 976–984.

(9) Frisch, M. J. ; Trucks, G. W.; Schlegel, H. B.; Scuseria, G. E.; Robb, M. A.; Cheeseman, J. R.; Montgomery, J. A., Jr.; Vreven, T.; Kudin, K. N.; Burant, J. C.; Millam, J. M.; Iyengar, S. S.; Tomasi, J.; Barone, V.; Mennucci, B.; Cossi, M.; Scalmani, G.; Rega, N.; Petersson, G. A.; Nakatsuji, H.; Hada, M.; Ehara, M.; Toyota, K.; Fukuda, R.; Hasegawa, J.; Ishida, M.; Nakajima, T.; Honda, Y.; Kitao, O.; Nakai, H.; Klene, M.; Li, X.; Knox, J. E.; Hratchian, H. P.; Cross, J. B.; Adamo, C.; Jaramillo, J.; Gomperts, R.; Stratmann, R. E.; Yazyev, O.; Austin, A. J.; Cammi, R.; Pomelli, C.; Ochterski, J. W.; Ayala, P. Y; Morokuma, K.; Voth, G. A.; Salvador, P.; Dannenberg, J. J.; Zakrzewski, V. G.; Dapprich, S.; Daniels, A. D.; Strain, M. C.; Farkas, O.; Malick, D. K.; Rabuck, A. D.; Raghavachari, J. B.; Foresman, J. V.; Ortiz, Q.; Cui, A. G.; Baboul, S.; Clifford, J.; Cioslowski, B. B.; Stefanov, K.; Liu, G.; Liashenko, A.; Piskorz, P.; Komaromi, I.; Martin, R. L.; Fox, D. J.; Keith, T.; Al-Laham, M. A.; Peng, C. Y.; Nanayakkara, A.; Challacombe, M.; Gill, P. M. W.; Johnson, B.; Chen, W.; Wong, M. W.; Gonzalez, C.; Pople, J. A. *GAUSSIAN 03*, Revision A.1,Gaussian, Inc.: Pittsburgh, PA, 2003.

(10) (a) Würtner, F.; Ahmet, S.; Thalacker, C.; Debaerdemaecker, T. *Chem.—Eur. J.* **2002**, *8*, 4742–4750. (b) Chopin, S.; Chaignon, F.; Blart, E.; Odobel, F. *J. Mater. Chem.* **2007**, *17*, 4139–4146.

(11) (a) Kruger, H.; Janietz, S.; Sainova, D.; Dobreva, D.; Koch, N.; Vollmer, A. *Adv. Funct. Mater.* **2007**, *17*, 3715–3723. (b) Guo, X.; Warson, M. D. *Org. Lett.* **2008**, *10*, 5333–5336. (c) Piyakulawat, P.; Keawprajak, A.; Chindaduang, A.; Hanusch, M.; Asawapirom, U. *Synth. Met.* **2009**, *159*, 467–472. (d) Chen, S.; Liu, Y.; Qiu, W.; Sun, X.; Ma, Y.; Zhu, D. *Chem. Mater.* **2005**, *17*, 2208–2215. (e) Huang, J.; Fu, H.; Wu, Y.; Chen, S.; Shen, F.; Zhao, X.; Liu, Y.; Yao, J. *J. Phys. Chem. C* **2008**, *112*, 2689–2696. (f) Chen, Z.; Zheng, Y.; Yan, H.; Facchetti, A. *J. Am. Chem. Soc.* **2009**, *131*, 8–9. (g) Yan, H.; Chen, Z.; Zheng, Y.; Newman, C.; Quinn, J. R.; Dötz, Kastler, F.; Facchetti, A. *Nature* **2009**, *457*, 667–687.

(12) Lee, S. K.; Zu, Y.; Herrmann, A.; Geerts, Y.; Mullen, K.; Bard, A. J. *J. Am. Chem. Soc.* **1999**, *121*, 3513–3530.

(13) (a) Alp, S.; Erten, S.; Karapire, C.; Koz, B.; Doroshenko, A. O.; Icli, S. *J. Photochem. Photobiol., A* **2000**, *135*, 103–110. (b) Erten, S.; Alp, S.; Icli, S. *J. Photochem. Photobiol., A* **2005**, *175*, 214–220. (c) Langhals, H.; Jaschke, H. *Chem.—Eur. J.* **2006**, *12*, 2815–2824. (d) Adachi, M.; Murata, Y.; Nakamura, S. *J. Phys. Chem.* **1995**, *99*, 14240–14246.

(14) Speight, J. G. *Lange's Handbook of Chemistry*, 16th ed.; McGraw-Hill: New York, 2005.

(15) Lukeš, V.; Matuszná, K.; Rapta, P.; Šolc, R.; Dunsch, L.; Aquino, A. J. A.; Lischka, H. *J. Phys. Chem. C* **2008**, *112*, 3949.

(16) (a) Jones, B. A.; Facchetti, A.; Wasielewski, M. R.; Marks, T. J. *J. Am. Chem. Soc.* **2007**, *129*, 15259–15278. (b) Cervini, M.; Li, X. C.; Spencer, G. W. C.; Holmes, A. B.; Moratti, S. C.; Friend, R. *Synth. Met.* **1997**, *84*, 359–360. (c) Li, Y.; Cao, Y.; Wamg, D.; Yu, G.; Heeger, A. J. *Synth. Met.* **1997**, *99*, 243–248. (d) Singh, T. B.; Erten, S.; Gunes, S.; Zafer, C.; Turkmen, G.; Kuban, B.; Teoman, Y.; Sariciftci, S.; Icli, S. *Org. Electron.* **2006**, *7*, 480–489.

(17) (a) Boudinet, D.; Blevennec, G. L.; Serbutoviez, C.; Verilhac, J.-M.; Yan, H.; Horowitz, G. *J. Appl. Phys.* **2009**, *105*, 084510. (b) Yang, D.; Shrestha, R. P.; Li, Y. X.; Yan, L.; Irene, E. A. *J. Vac. Sci. Technol., B* **2006**, *24*, 2653–2658.

JP908931W